ISSN(Online): 2320-9801
ISSN (Print): 2320-9798

International Journal of Innovative Research in Computer and Communication Engineering

(An ISO 3297: 2007 Certified Organization)

Vol. 3, Issue 8, August 2015

Capacitance Modeling of AlN dielectric for AlGaN HEMT (MIS-HEMT) Device with two Subbands

S.Baskaran [1], P.Kalaivani[2], M.Naveenkumar[3]

Professor, Department of Electronics and Communication Engineering, SKP Engineering College Tiruvannamalai, Tamilnadu, India[1]

Assistant Professor, Department of Electronics and Communication Engineering, SKP Engineering College Tiruvannamalai, Tamilnadu, India[2, 3]

ABSTRACT: This paper presents a physics-based model for two-dimensional electron gas (2DEG) density of $Al_xGa_{1-x}N$/GaN MIS-HEMT device with AlN dielectric. With the unified E_f model, a surface-potential (ϕ_s) based continuous and symmetric drain current (I_{ds}) model is developed. Using the unified single-piece explicit(E_f) solution, from sub-threshold to strong inversion region, an accurate and simple charge control model for the metal–insulator–semiconductor high electron-mobility transistor (MISHEMT) device is formulated which includes the two lowest sub-bands (E_0 and E_1) in the triangular well. Based on this, the gate charge, and the gate capacitances have been developed. The modeled I-V and C-V characteristics of the device are validated by comparison with the experimental data. The proposed model is in very good agreement with numerical calculations.

KEYWORDS: GaN, 2-Dimensional electron gas (2DEG) density, metal–insulator–semiconductor high electron-mobility transistor (MISHEMT), triangular quantum well, DC characteristics model, and Capacitance model.

I. INTRODUCTION

AlGaN/GaN based high electron mobility transistors (HEMTs) delivers outstanding performance such as high electron mobility, high saturation current, low on-resistance and large breakdown voltage. These unique properties make AlGaN/GaN HEMTs a promising candidate for high frequency, high speed and nanoscale power applications [1]. The wide bandgap and high breakdown voltage of AlGaN/GaN materials limit the performance and reliability of AlGaN/GaN HEMTs for operation in high temperature environments [2]. The primary performance limiting factor of AlGaN/GaN HEMTs is current collapse effect. Current collapse effect is recognized as a foremost aspect causing DC and RF parameters degradation under large input signals. The performance of AlGaN/GaN HEMTs for high power and high temperature applications can be improved by using insulating gate dielectrics. The insulating dielectrics are extensively used to reduce gate leakage current, enhance operating voltage and shield device surface. The oxide-based dielectrics pave way for interface sources leading to current collapse. With this consideration, the nitride-based dielectrics especially AlN are more preferred due to the larger band gap and smaller mismatch [3]. Even though HEMTs possess many benefits, but when compared with metal-insulator-semiconductor high electron-mobility transistor (MIS-HEMT), HEMTs

lags in some factors. MIS-HEMTs have attracted a lot of attention due to much reduced gate leakage and better restrain of current collapse.

In this paper, a physics-based two dimensional electron gas (2DEG) density (n_s) model for $Al_xGa_{1-x}N$/GaN MIS-HEMT device with AlN dielectric is presented. With the proposed n_s model, a surface-potential (ϕ_s) based continuous and symmetric drain current (I_{ds}) model is developed. Using the unified single-piece explicit (E_f) solution, an accurate and a simple charge control model for $Al_xGa_{1-x}N$ /AlN/GaN MIS-HEMT device is formulated which includes the two lowest sub-bands (E_0 and E_1) in the triangular well. The proposed model results are verified with the experimental data.

DOI: 10.15680/IJIRCCE.2015. 0308143

ISSN(Online): 2320-9801
ISSN (Print): 2320-9798

International Journal of Innovative Research in Computer and Communication Engineering

(An ISO 3297: 2007 Certified Organization)

Vol. 3, Issue 8, August 2015

2DEG	Two-dimensional electron gas
UID	Unintentionally doped
$\varepsilon_{\text{AlGaN}}$	Permittivity or dielectric constant of AlGaN
ε_{AlN}	Permittivity or dielectric constant of AlN
d_d	Thickness of AlGaN barrier layer
d_i	Thickness of AlN spacer layer
$d = d_d + d_i$	Total thickness of AlGaN barrier and AlN Spacer layer
$\Delta E_{c,eff}$	Conduction band offset
N_b	Doping concentration in AlGaN
σ	Polarization induced charge density
μ_0	Low- filed mobility
n_s	Sheet Carrier density
V_{th}	Thermal voltage
C_g	Gate capacitance
λ	Channel length modulation parameter
D	Density of states
q	Electron charge
K	Boltzmann’s constant
E_0, E_1	Formation of first and second Energy sub-bands
γ_0, γ_1	Experimentally determined parameters using AlGaN effective mass

Model structure and Formulation

The schematic representation of the $Al_xGa_{1-x}N$/AlN/GaN MIS-HEMT is shown in Fig.1 and the corresponding band diagram of MIS HEMT including the first two subbands is shown in Fig.2.

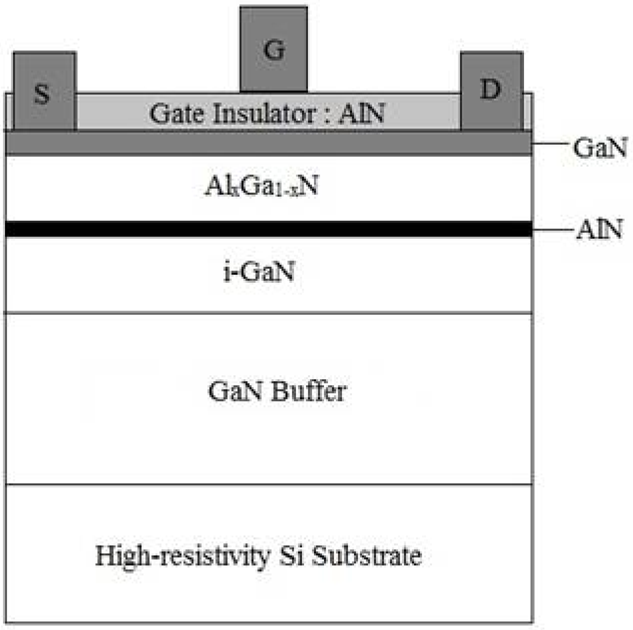

Fig.1 Schematic cross-section of $Al_xGa_{1-x}N$/AlN/GaN MIS-HEMT

The measured device is with a source-gate spacing L_{GS} of 1µm, gate length L_G of 2.5 µm, drain-gate spacing L_{GD} of 6µm and gate width of 60 µm. Also it consists of high resistivity Si wafer over 2.5 µm carbon- doped GaN buffer layer, 500-nm i-GaN layer, 1-nm AlN interlayer, 23-nm undoped $Al_{0.25}Ga_{0.75}N$ top barrier layer, and 5-nm GaN cap layer.

The Fermi potential (in volts), E_f, is referenced to the conduction-band edge at the heterointerface (x = 0). Electrostatic potential and voltage (in volts) are referenced to the Fermi level in the body.

The analytical expression of n_s with two sub-bands in the quantum well given by [1]

$$n_s = Dv_{th} \ln\left[\left(1+e^{(E_f-E_0)/v_{th}}\right)\left(1+e^{(E_f-E_1)/v_{th}}\right)\right] \tag{1}$$

$$E_0 = \gamma_0 n_s^{2/3} \tag{1a}$$

$$E_1 = \gamma_1 n_s^{2/3} \tag{1b}$$

where D is the density of states of the 2DEG associated with a single quantized energy level, with E_0 and E_1 being the two lowest sub-bands in the triangular well with respect to the conduction-band edge at the heterointerface, V_{th} = kT/q is the thermal voltage and E_f is the Fermi level of the bottom of the triangular well.

On the other hand, a self consistent solution of n_s considering two energy levels is [4]

$$n_s = DV_{th}\left\{\ln\left[\exp\left(\frac{E_f - E_o}{V_{th}}\right)+1\right]+\ln\left[\exp\left(\frac{E_f - E_1}{V_{th}}\right)+1\right]\right\} \tag{2}$$

where

$$E_0 = \gamma_0 n_s^{2/3}$$
$$E_1 = \gamma_1 n_s^{2/3}$$

$$n_s = \frac{\varepsilon}{qd}\left(V_{g_o} - E_f - V_x\right) \tag{3}$$

where $V_{g_o} = V_g - V_{off}$, V_{off} is cutoff voltage, V_x is the channel potential at any point x in the channel.

$$n_s = \frac{\varepsilon(x)}{q(d_d + d_i)}(V_{gs} - V_{off} - V_x - E_f) \tag{4}$$

where, $\varepsilon(x)$ is the total permittivity of AlGaN and AlN, $d=d_d+d_i$ is the total thickness of barrier AlGaN and spacer AlN.

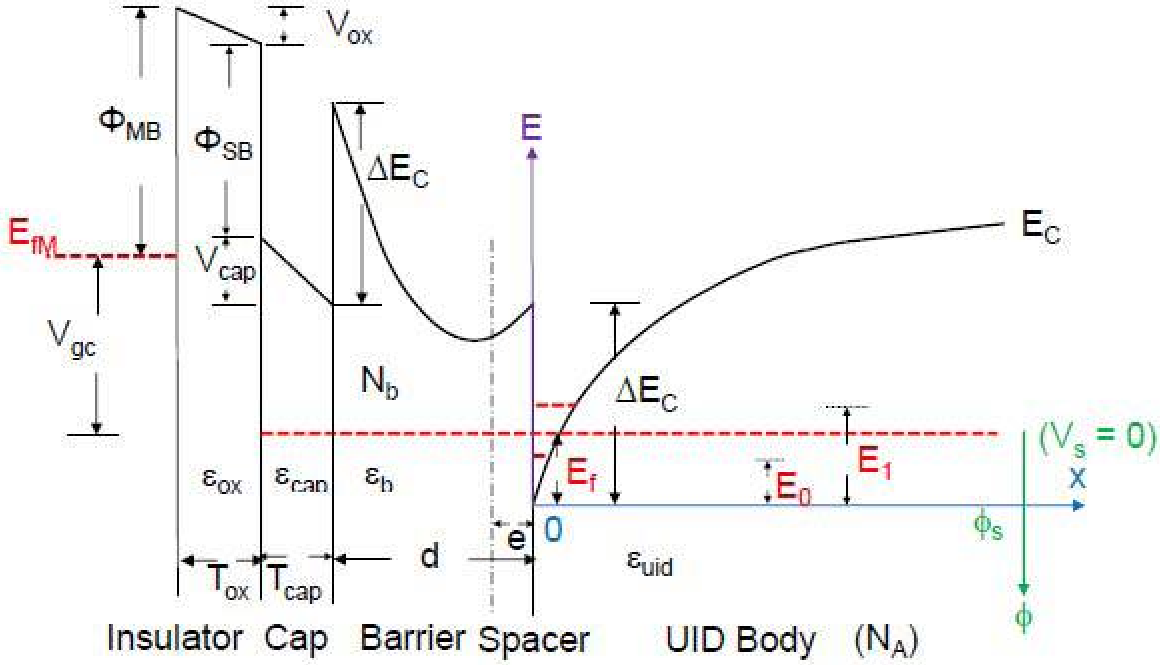

Fig.2 Energy-band diagram of a generic heterostructure MIS-HEMT

The parameters and description of all the other symbols used is given in Table 1. For the purpose of developing a compact drain model, a continuous unified expression for n_s valid in all regions of operation is desirable [5].

In this work, we have made an analysis and modeled sheet carrier density n_s and core drain model with respect to gate voltage V_{gs}, gate capacitance C_g, and also explored the DC characteristics model for insulator layer based $Al_xGa_{1-x}N$/AlN/GaN MIS HEMTs. All the results are validated using experimental data. This model is developed by considering the variation of E_f, the first subband E_0, the second subband E_1 and n_s with applied gate voltage V_g.

a) Analysis of 2DEG n_s Model

Unified Single-Piece E_f Solution:

A unified single-piece E_f is derived [1] can be written as

$$E_f(V_g, V_c) = V_{go} - \Delta E_f \tag{5}$$

where

$$\Delta E_f = \frac{2v_{th}\left(1-\frac{E_{f,act}}{V_{go,act}}\right)\ln\left(1+\exp\left(\frac{V_{go}}{2v_{th}}\right)\right)}{1 + \tilde{C}_d\left(1-\frac{E_{f,act}}{V_{go,act}}\right)\exp\left(-\frac{V_{go}}{2v_{th}}\right)} \tag{6}$$

$E_{f,act}$ is valid from moderate to strong inversion regions namely active region [1].

$$E_{f,act} = \frac{2M_{eff}V_{go,CR}\,ln\left(1+exp\left(\frac{V_{g0}}{2V_{g0,CR}}\right)\right)}{1+\eta\frac{M_{eff}V_{g0,CR}}{E_{f,mod}}exp\left(\frac{-V_{g0}}{2V_{g0,CR}}\right)} \tag{7}$$

where η is a fitting parameter, $V_{g0,CR}$ is defined as critical voltage, $E_{f,mod}$is the unified E_f value in moderate to strong inversion region.

In moderate inversion region, the accuracy is not very much demand, therefore ΔE_f can be written as [1]

$$\Delta E_f = \frac{2v_{th}\left(1-M_{eff}\right)\ln\left(1+e^{V_{go}/2v_{th}}\right)}{1 + \tilde{C}_d\left(1-M_{eff}\right)e^{-V_{go}/2v_{th}}} \tag{8}$$

b) Drain-Current Model

Once an explicit E_f model is developed, a compact surface potential model can be used in $\phi_s$based terminal current/charge model. We use MOSFET model for generic MISHEMTs, treating the 2DEG as an inversion charge sheet on a UID body. The major relevant formulas are listed in the following.

The drain current is given by [1]

$$I_{ds} = \mu_{eff}C_d\frac{W}{L}\left(V_g - V_{off} - \bar{\phi}_s - 2v_{th}\right)V_{ds,eff} \tag{9}$$

where W and L are width and length of the gate.

$$\bar{\phi}_s = \left(\phi_{s,s} + \phi_{s,d}\right)/2 \tag{10}$$

$$\begin{aligned}\phi_{s,c} &= V_{c,eff} + E_f\left(V_{c,eff}\right)\\ &= V_g - V_{off} - \Delta E_f\left(V_{c,eff}\right) \qquad (c = s,\ d)\end{aligned} \tag{11}$$

where $\phi_{s,c} \equiv \phi_s\left(V_{c,eff}\right)$ with c=s/d for source/drain (S/D)

DOI: 10.15680/IJIRCCE.2015. 0308143

The effective source–drain voltage is given by [1]

$$V_{ds,eff} = V_{d,eff} - V_{s,eff} \tag{12}$$

$$V_{c,eff} = \vartheta\left\{V_{c,sat}, V_c; \delta\right\} \tag{13}$$

$$V_{d,sat} = \frac{V_{gt}(V_s)E_{sat,s}L}{V_{gt}(V_s) + E_{sat,s}L + 4v_{th}} + V_s \tag{14}$$

$$V_{s,sat} = \frac{V_{gt}(V_d)E_{sat,d}L}{V_{gt}(V_d) + E_{sat,d}L + 4v_{th}} + V_d \tag{15}$$

$$E_{sat,c} = 2v_{sat} / \mu_{0,c} \tag{16}$$

where V_{sat} is the saturation velocity.

The vertical-field mobility is given by

$$\mu_0 = \frac{\mu_1}{1 + \frac{\mu_1}{\mu_2} E_{eff}^{1/3} + \frac{\mu_1}{\mu_3} E_{eff}^{2}} \tag{17}$$

where μ_1, μ_2, μ_3 are mobility parameters.
The another formula from MOSFETs is the 2DEG charge, given by qn_s / C_d from (1) as

$$V_{gt}(V_c) = V_g - V_{off} - \bar{\phi}_s(V_c) \tag{18}$$

Also

$$V_{gt}(V_c) = \Delta E_f\left(V_c\right) \tag{19}$$

The effective field used in the vertical-field mobility is given by

$$E_{eff} = \frac{C_d\left(V_g - V_{off} - \bar{\phi}_s\right)}{2\varepsilon_{uid}}$$

$$= C_d \frac{\overline{\Delta E_f\left(V_{c,eff}\right)}}{2\varepsilon_{uid}} \tag{20}$$

$$\overline{\Delta E_f\left(V_{c,eff}\right)} = \frac{\Delta E_f\left(V_{s,eff}\right) + \Delta E_f\left(V_{d,eff}\right)}{2} \tag{21}$$

where $\Delta E_f(V_c)$ is (6)

c) Charge Model

When the gate depletion and channel depletion overlap to give a fully depleted barrier layer, the carrier density is given by [4]

$$n_s = \frac{\varepsilon}{qd}\left(V_{go} - E_f\right) \tag{22}$$

where Vg0 = Vg – V_{OFF}.

$$V_{go} - V = \frac{n_s qd}{\varepsilon} + \frac{\gamma_0 + \gamma_1}{2} n_s^{2/3} + \frac{V_{th}}{2} \ln\left(\frac{n_s}{DV_{th}}\right) \tag{23}$$

An analytical current model can be formulated using the definition of the drain current along the channel is

$$dV = -\left(\frac{qd}{\varepsilon} + \frac{\gamma_0 + \gamma_1}{3} n_s^{-1/3} + \frac{V_{th}}{2} n_s^{-1}\right) dn_s \tag{24}$$

The gate charge can be obtained by integrating the charge density along the channel over the gate area

$$Q_G = W \int_0^L q n_s(x)\, dx \tag{25}$$

$$Q_G = WLq \left(\frac{\int_{V_s}^{V_d} n_s^2 dV}{\int_{V_s}^{V_d} n_s dV} \right) \tag{26}$$

The two integrals at the numerator and denominator is represented as f(n_s) and g(n_s), respectively, and integrating after changing the integration variable using (23) gives

$$f(n_s) = \frac{qd}{3\varepsilon}\left(n_D^3 - n_S^3\right) + \frac{\gamma_0 + \gamma_1}{8}\left(n_D^{8/3} - n_S^{8/3}\right) + \frac{1}{4} V_{th}\left(n_D^2 - n_S^2\right) \tag{27}$$

$$g(n_s) = \frac{qd}{2\varepsilon}\left(n_D^2 - n_S^2\right) + \frac{\gamma_0 + \gamma_1}{5}\left(n_D^{5/3} - n_S^{5/3}\right) + \frac{1}{2} V_{th}\left(n_D - n_S\right) \tag{28}$$

The total gate charge then becomes

$$Q_G = WLq \left(\frac{\frac{qd}{3\varepsilon}\left(n_D^3 - n_S^3\right) + \frac{\gamma_0 + \gamma_1}{8}\left(n_D^{8/3} - n_S^{8/3}\right) + \frac{1}{4} V_{th}\left(n_D^2 - n_S^2\right)}{\frac{qd}{2\varepsilon}\left(n_D^2 - n_S^2\right) + \frac{\gamma_0 + \gamma_1}{5}\left(n_D^{5/3} - n_S^{5/3}\right) + \frac{1}{2} V_{th}\left(n_D - n_S\right)} \right) \tag{29}$$

d) Capacitance model

The gate-source and gate-drain capacitances can now be calculated using the partial differentiations of the gate charge with respect to the corresponding source and drain terminal voltages. Therefore the capacitances are obtained as

$$C_{Gx} = WLq \left(\frac{\frac{\partial f(n_S)}{\partial V_x} g(n_S) - f(n_S) \frac{\partial g(n_S)}{\partial V_x}}{g(n_S)^2} \right) \tag{30}$$

f(n_s) and g(n_s) can also be defined as

$$f(n_s) = f_{main}(n_D) - f_{main}(n_S) \tag{31}$$

$$g(n_s) = g_{main}(n_D) - g_{main}(n_S) \tag{32}$$

where

$$f_{main}(n_x) = \frac{qd}{3\varepsilon}\left(n_x^3\right) + \frac{\gamma_0+\gamma_1}{8}\left(n_x^{8/3}\right) + \frac{1}{4}V_{th}\left(n_x^2\right) \tag{33}$$

$$g_{main}(n_x) = \frac{qd}{2\varepsilon}\left(n_x^2\right) + \frac{\gamma_0+\gamma_1}{5}\left(n_x^{5/3}\right) + \frac{1}{2}V_{th}\left(n_x\right) \tag{34}$$

where $n_x = n_D$ at the drain terminal and $n_x = n_S$ at the source terminal.

From (33) and (34), the derivatives of $f_{main}(n_x)$ and $g_{main}(n_x)$ can be written as

$$\frac{df_{main}(n_x)}{dV_x} = \left(\frac{qd}{\varepsilon}\left(n_x^2\right) + \frac{\gamma_0+\gamma_1}{3}\left(n_x^{5/3}\right) + \frac{1}{2}V_{th}\left(n_x\right)\right)\frac{dn_x}{dV_x} \tag{35}$$

$$\frac{dg_{main}(n_x)}{dV_x} = \left(\frac{qd}{\varepsilon}\left(n_x\right) + \frac{\gamma_0+\gamma_1}{3}\left(n_x^{2/3}\right) + \frac{1}{2}V_{th}\right)\frac{dn_x}{dV_x} \tag{36}$$

where the factor dn_x / dV_x can be obtained from (27).

Therefore, the gate-source and the gate-drain capacitances can now be expressed as

$$\mathrm{C}_{\mathrm{Gx}} = \mathrm{WLq}\left(\frac{\dfrac{df_{main}(n_x)}{dV_x}\, g\left(n_s\right) - f\left(n_s\right)\dfrac{dg_{main}(n_x)}{dV_x}}{\left(g\left(n_s\right)\right)^2}\right) \tag{37}$$

IV. RESULTS AND DISCUSSION

The key transport for HEMT devices is mainly by the 2DEG charge density. The 2DEG charge density (1) with two sub-bands E_0 and E_1 in the triangular well approximation is a good model. The proposed model results are compared against experimental data [5] which shows an excellent agreement between them in the applied voltage of device operation.

Fig.3 shows the 2DEG sheet carrier density n_s obtained by our model (4). The obtained result is compared with the experimental result [5] shows excellent agreement and the peak values of both proposed and experimental n_s are mentioned in the figure. From the graph it is clear that there is the occurrence of linear relationship between n_s and V_{gs} when the device gets turned on completely. Further increase in V_{gs} makes the 2DEG density to reach its maximum and keeps constant. This transformation of n_s is due to the thickness of the barrier AlGaN (d_d) and spacer AlN (d_i). The higher mole fraction of Al will lead to the higher sheet carrier density.

Fig.4 shows the output characteristics of $Al_xGa_{1-x}N$/AlN/GaN MISHEMT under drain bias. The obtained result has reproduced the output characteristics of device very well. The proposed model achieved smooth and accurate descriptions of I_{ds}-V_{ds} characteristics. From the plot, we can say that there is a good agreement between proposed model and experimental data [5]. The drain voltage is varied from -6V to +4V. Beyond V_{ds}=+4V, the drain current may suffer from the electric field-related mobility degradation [5].

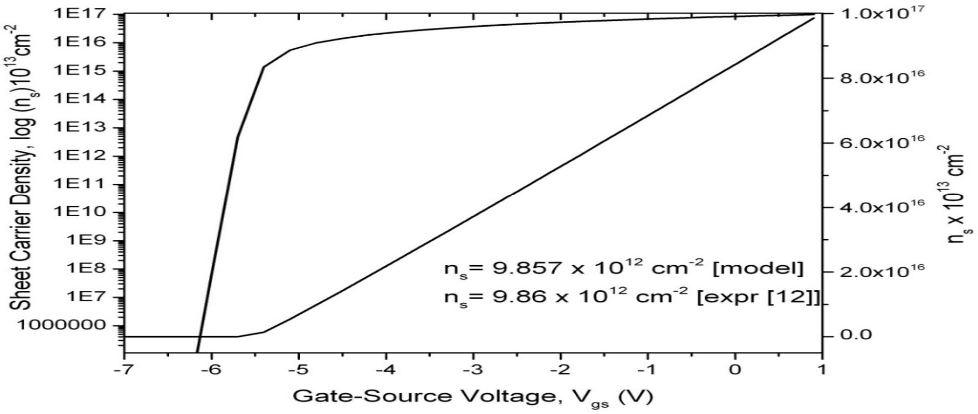

Fig.3 Variation of Sheet carrier density n_s with respect to gate-to-source voltage V_{gs} with T=300K for $Al_{0.3}Ga_{0.7}N$/GaN AlN-MISHEMT. The thickness of AlGaN barrier and AlN Spacer is d=24nm and V_{off} = -5.7V. Data plot n_s in both logarithm and linear scale is verified with experimental data [5].

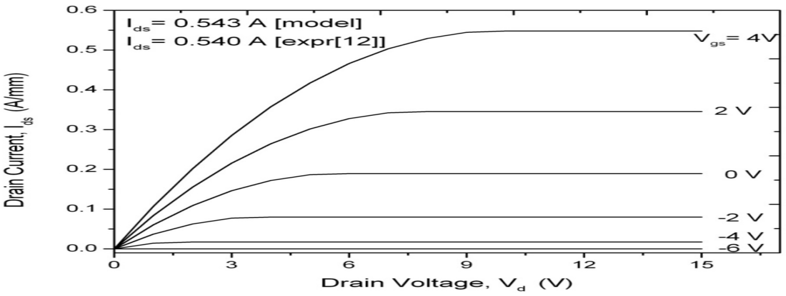

Fig.4 Modeled I_{ds} - V_{ds} characteristics of $Al_{0.3}Ga_{0.7}N$/GaN AlN-MISHEMT at various V_{gs} shown is compared with experimental data taken from [5].

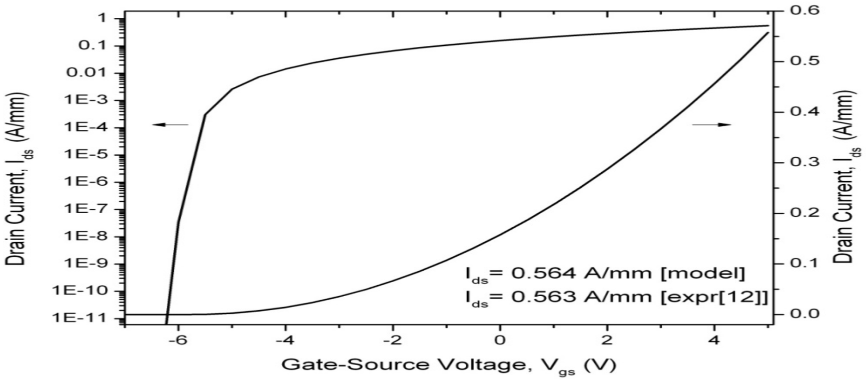

Fig.5 Comparison of modeled I_d-V_{gs} characteristics with experimental data for $Al_{0.3}Ga_{0.7}N$ MISHEMT with L_g=0.6µm and W=100µm device. Experimental data is taken from [5].

Fig.5 shows the transfer characteristics of $Al_xGa_{1-x}N$/AlN/GaN MISHEMT. The The variation of the drain current (I_{ds}) with gate to source voltage (V_{gs}) shows very considerable I_{ds}-V_{gs} relationship of the device. The drain current has a maximum current of 0.564 A/mm. The maximum drain current value of the proposed model and the experimental data is mentioned in the figure. The AlN/GaN hetero-junction interface polarization charge has some effect influence on transfer characteristics and improves the drain current [6].

Fig.6 shows the plot of gate to source capacitance with gate to source voltage. The variation of gate to source capacitance C_{gs} with gate to source voltage V_{gs} shows good agreement with the experimental data [5]. When the device is in OFF state, there is no contribution from C_{gs}, this is because of the very low 2DEG density. When the device is turned ON, there is a rapid increasing of Cgs due to the accumulation of positive charges by gate. As the gate to source voltage increases furthermore, the C_{gs} gets increases linearly and then keep unchanging. The presence of AlN dielectric caused the gate capacitance to contribute significantly. The thinner the dielectric layer will cause the greater gate capacitance [2].

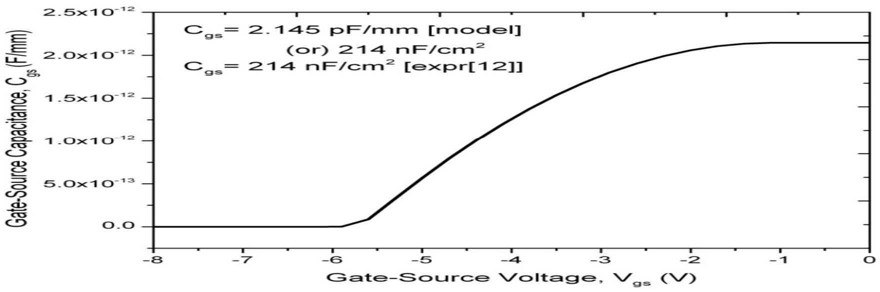

Fig.6 Modeled gate-to-source Capacitance, C_{gs} of a device versus gate voltage in which the operating region consists of the two lowest sub-bands (E_0 and E_1) in the triangular well, at a drain voltage of 15 V, (data from [5]).

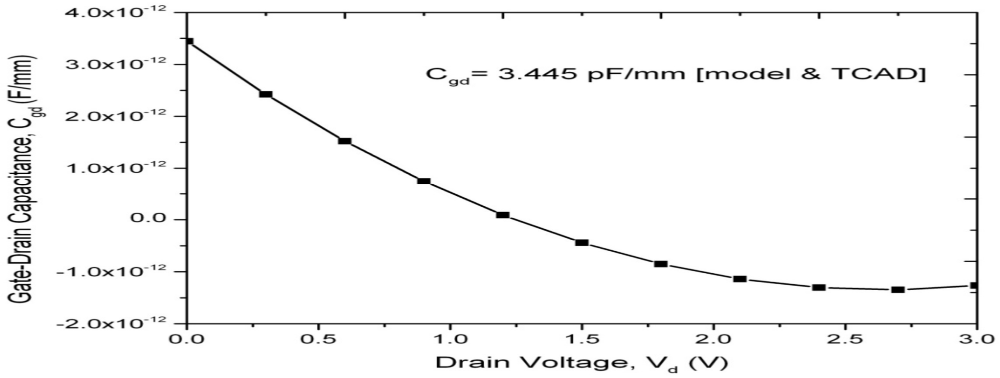

Fig.7 Variation of gate-to-drain capacitance, C_{gd} with drain voltage, at a gate voltage of -1V.

Fig.7 shows the simulated and modeled gate-drain capacitance C_{gd} versus drain voltage V_d. The gate voltage is kept stable to -1V. The simulation of C_{gd} is done using TCAD. The result shows that the simulation data and modeled data of C_{gd} versus V_d matched well. The C_{gd} converges gradually to a constant value when V_d increases, which means that V_{ds} will affect the channel charge a little when the device is saturated [7].

V. CONCLUSION

Simple physics-based models for two-dimensional electron gas (2DEG) density, a surface potential based drain current, gate charge and capacitances of $Al_xGa_{1-x}N$/AlN/GaN MISHEMT have been presented. They are developed from a unified E_f model by considering the two lowest subbands (E_0 and E_1) in the triangular well. This consideration resulted in simple and distinct models for 2DEG density, drain current, gate charge and capacitances. These models obtained an excellent agreement between modeled and experimental data for generic $Al_xGa_{1-x}N$/AlN/GaN MISHEMT, by sustaining a fine level of accuracy for 2DEG density, I-V and C-V characteristics. Due to the presence of AlN dielectric, current collapse effect is reduced considerably. Thus the model can be utilized efficiently when resolving device behavior even in high temperature environments.

REFERENCES

[1] J. Zhang, B. Syamal, Xing Zhou, S. Arulkumaran, and Geok Ing Ng, “A Compact Model for Generic MIS-HEMTs Based on the Unified 2DEG Density Expression,” IEEE Trans. Electron Devices, vol. 61, no. 2, Feb. 2014.
[2] Zhiwei Bi, Yue Hao, “Characteristics analysis of Gate Dielectrics AlGaN/GaN MIS-HEMT,” 2009 IEEE.
[3] Xiao-Yong Liu, S. Zhao, L. Zhang, H. Huang, Jin-Shan Shi, Chun-Min Zhang, H. Lu, P. Wang and David Wei Zhang, “AlGaN/GaN MISHEMTs with AlN gate dielectric grown by thermal ALD technique,” Liu et al. Nanoscale Research Letters, 2015.
[4] S. Khandelwal, T.A. Fjeldly, “A physics based compact model of I–V and C–V characteristics in AlGaN/GaN HEMT devices,” Solid-State Electronics, May. 2012.
[5] F. M. Yigletu, S. Khandelwal, Tor A. Fjeldly, Fellow, and B. Iñiguez, “Compact Charge-Based Physical Models for Current and Capacitances in AlGaN/GaN HEMTs,” IEEE Trans. Electron Devices, 2013.
[6] Wang Jie, Sun Lingling, Liu Jun, and Zhou Mingzhu, “A surface-potential-based model for AlGaN/AlN/GaN HEMT”, Journal of Semiconductors, Sep 2013, Vol. 34, No. 9.
[7] X. Cheng, M. Li, and Y. Wang, “Physics-based compact model for AlGaN/GaN MODFETs with close-formed I–V and C–V characteristics,” IEEE Trans. Electron Devices, vol. 56, no. 12, pp. 2881–2887, Dec. 2009.
[8] Mishra UK, Shen L, Kazior TE, Yi-Feng W, “GaN-based RF power devices and amplifiers,” Proc IEEE. 2008; 96:287–305.
[9] J. Zhang, B. Syamal, Xing Zhou, S. Arulkumaran, and Geok Ing Ng, “A Compact Model for Generic MIS-HEMTs Based on the Unified 2DEG Density Expression,” IEEE Trans. Electron Devices, vol. 61, no. 2, Feb. 2014.
[10] D. Delagebeaudeuf and N. T. Linh, “Metal-(n) AlGaAs-GaAs two dimensional electron gas FET,” IEEE Trans. Electron Devices, vol. 29, no. 6, Jun. 1982.